



OPEN

# Lysine pyrrolation is a naturally-occurring covalent modification involved in the production of DNA mimic proteins

SUBJECT AREAS:

CHEMICAL  
MODIFICATION

DIAGNOSTIC MARKERS

Received

16 April 2014

Accepted

28 May 2014

Published

18 June 2014

Hiroaki Miyashita<sup>1</sup>, Miho Chikazawa<sup>1</sup>, Natsuki Otaki<sup>1</sup>, Yusuke Hioki<sup>1</sup>, Yuki Shimozu<sup>1</sup>, Fumie Nakashima<sup>1</sup>, Takahiro Shibata<sup>1,2</sup>, Yoshihisa Hagihara<sup>3</sup>, Shoichi Maruyama<sup>4</sup>, Noriyoshi Matsumi<sup>5</sup> & Koji Uchida<sup>1</sup>

<sup>1</sup>Graduate School of Bioagricultural Sciences, Nagoya University, Nagoya 464-8601, Japan, <sup>2</sup>PRESTO, Japan Science and Technology Agency (JST), Kawaguchi, Saitama 332-0012, Japan, <sup>3</sup>National Institute of Advanced Industrial Science and Technology (AIST), Ikeda, Osaka 563-8577, Japan, <sup>4</sup>Department of Nephrology, Graduate School of Medical Sciences, Nagoya University, Nagoya 466-8550, Japan, <sup>5</sup>School of Materials Science, Japan Advanced Institute of Science and Technology, Ishikawa 923-1292, Japan.

Correspondence and requests for materials should be addressed to K.U. (uchidak@agr.nagoya-u.ac.jp)

**Covalent modification of proteins exerts significant effects on their chemical properties and has important functional and regulatory consequences. We now report the identification and verification of an electrically-active form of modified proteins recognized by a group of small molecules commonly used to interact with DNA. This previously unreported property of proteins was initially discovered when the  $\gamma$ -ketoaldehydes were identified as a source of the proteins stained by the DNA intercalators. Using 1,4-butanediol, the simplest  $\gamma$ -ketoaldehyde, we characterized the structural and chemical criteria governing the recognition of the modified proteins by the DNA intercalators and identified *N*<sup>ε</sup>-pyrrolylysine as a key adduct. Unexpectedly, the pyrrolation conferred an electronegativity and electronic properties on the proteins that potentially constitute an electrical mimic to the DNA. In addition, we found that the pyrrolated proteins indeed triggered an autoimmune response and that the production of specific antibodies against the pyrrolated proteins was accelerated in human systemic lupus erythematosus. These findings and the apparent high abundance of *N*<sup>ε</sup>-pyrrolylysine *in vivo* suggest that protein pyrrolation could be an endogenous source of DNA mimic proteins, providing a possible link connecting protein turnover and immune disorders.**

It is estimated that most of the proteins in the human body are post-translationally modified. Such modifications include phosphorylation, methylation, glycosylation, etc. They are enzyme-mediated and homeostatically important, either to carry out a specific structural or functional role or to allow the efficient recycling of the amino acid constituents. The post-translational modifications of proteins are some of the most efficient biological mechanisms for expanding the genetic code and for regulating cellular physiology. The covalent modifications of proteins are typically introduced onto proteins by enzyme-catalyzed processes, but can also result from enzyme-independent interactions between reactive metabolites and nucleophilic residues<sup>1</sup>, such as the side chain of lysine, one of the three basic residues critical for protein structure and function. Post-translational modifications of lysine residues have proven to be major regulators of gene expressions, protein-protein interactions, and protein processing and degradation.

It has been suggested that many of the effects of cellular dysfunction under oxidative stress are mediated by the products of the non-enzymatic reactions, such as the peroxidative degradation of polyunsaturated fatty acids<sup>2,3</sup>. Some of the lipid peroxidation products exhibit a facile reactivity with proteins, generating a variety of oxidation-associated molecular patterns that include intra- and intermolecular covalent adducts. Such molecular patterns could be the targets of B cell-mediated immune responses and induce T cell responses and add to the potential of certain aldehydes to induce an autoimmunity by breaking the B cell tolerance to non-modified proteins. The modification of self-proteins by lipid peroxidation products indeed results in reducing the tolerance to self-proteins<sup>4</sup>. It has also been proposed that the adducts, called oxidation-derived epitopes, generated on self-antigens are important immunodominant targets of natural antibodies (Abs) and suggested that these Abs play an important function in the host response to the consequences of oxidative stress during oxidative events that occur when cells undergo apoptosis<sup>5</sup>. These findings and the fact that the post-translational modification of proteins is enhanced during aging and in stressed cells, and arise under physiological conditions<sup>6,7</sup> suggest the existence of an association between the formation of covalently-modified proteins and immune disorders.

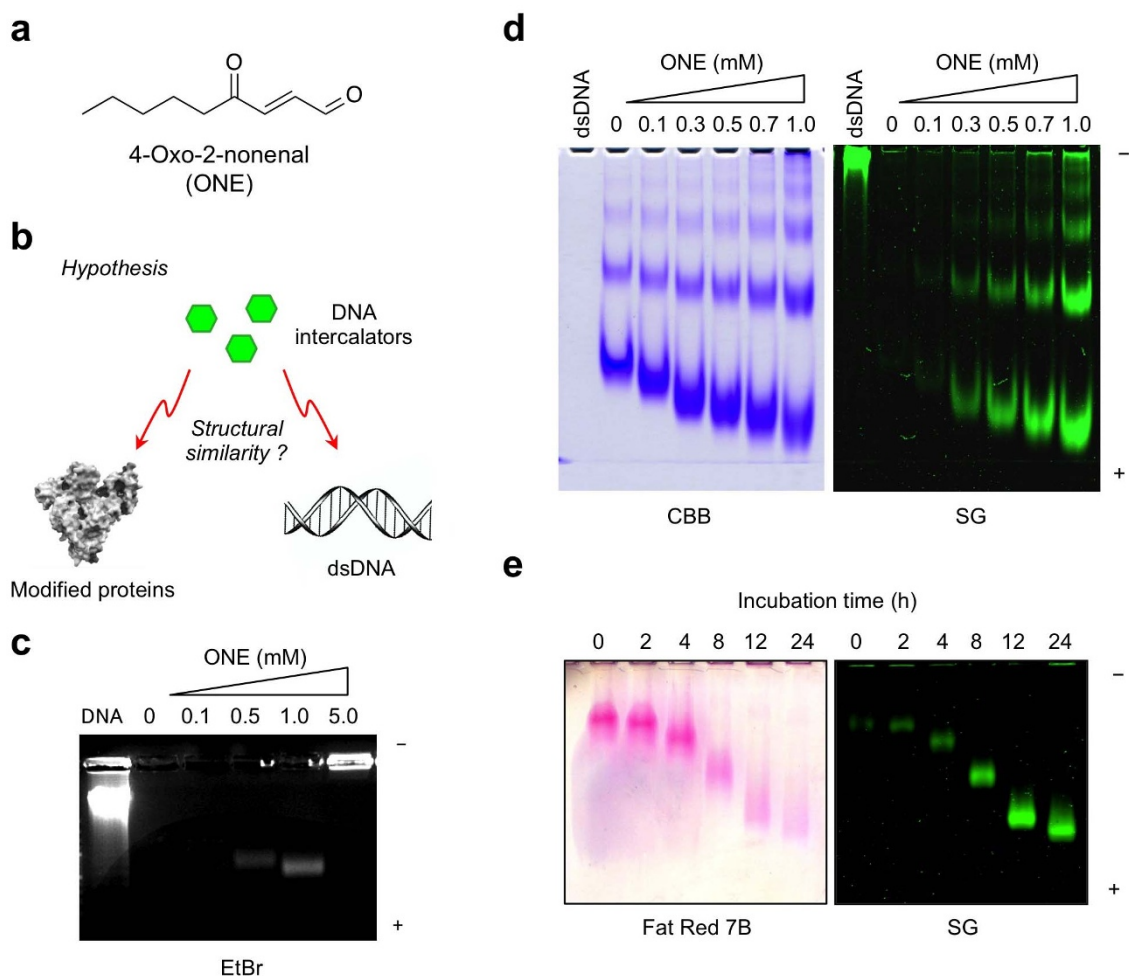


**Figure 1 | Recognition of ONE-modified proteins by DNA intercalators.** (a) Chemical structure of 4-oxo-2-nonenal (ONE). (b) A hypothesis for the recognition of ONE-modified proteins by DNA intercalators. (c) Binding of EtBr to the ONE-modified proteins. The ONE-modified proteins were prepared by incubating BSA (1.0 mg/ml) with ONE (0–5 mM) in PBS at 37°C for 24 h. Electrophoresis was performed in a 1% agarose gel. After electrophoresis, the gels were stained with EtBr. (d) Binding of SG to the ONE-modified proteins. The ONE-modified proteins were prepared by incubating BSA (1.0 mg/ml) with ONE (0–1 mM) in PBS at 37°C for 24 h. Electrophoresis was performed in a nondenaturing polyacrylamide gel. After electrophoresis, the gels were stained with CBB (*left*) and SG (*right*). (e) Recognition of oxidized LDL by SG. LDL (1 mg) was incubated with 5  $\mu\text{M}$   $\text{Cu}^{2+}$  in 1 ml of 50 mM PBS at 37°C. Agarose gel electrophoresis was performed with the Titan Gel lipoprotein system (Helena Laboratories, Saitama, Japan) for lipoprotein samples and the Titan Gel high-resolution protein system for protein samples. The samples were run on two separate gels. One gel was used for staining with Fat Red 7B (*left*) and the other was used for staining with SG.

A number of studies have shown that the anti-DNA autoantibodies (autoAbs) cross-react with a variety of antigens, including the intracellular and extracellular components. Some of the anti-DNA autoAbs, sharing structural similarities with the Abs against a bacterial polysaccharide, were shown to cross-react with the polysaccharide and protect mice against a lethal bacterial infection<sup>8,9</sup>. Other studies also demonstrated the cross-reactivity of the anti-DNA autoAbs with microbial protein antigens, non-nucleic acid autoantigens, cell membranes and extracellular matrix components<sup>10,11</sup>. In our previous study, to investigate whether lipid peroxidation is associated with the formation of autoantigenic proteins, we examined the cross-reactivity of protein-bound lipid peroxidation products with the sera from systemic lupus erythematosus (SLE)-prone mice, and identified 4-oxo-2-nonenal (ONE) (Fig. 1a), a  $\gamma$ -ketoaldehyde generated during the peroxidation of polyunsaturated fatty acids<sup>12</sup>, as a potential source of autoantigens<sup>13</sup>. In addition, following the identification of the active substance, we generated several anti-DNA monoclonal Abs (mAbs) from the SLE mice and observed that the mAbs showed a multi-specificity toward DNA and the ONE-modified proteins. However, the scope and broad functional significance of the antibody multi-specificity remain poorly understood. In this

context, we developed and examined the hypothesis (Fig. 1b) that the modified proteins might have structural properties similar to the double-stranded (ds) DNA.

## Results

**Identification of  $\gamma$ -ketoaldehyde-modified proteins as a target of DNA intercalators.** To determine the possibility of a structural similarity between dsDNA and the ONE-modified proteins, a group of small molecules (Fig. S1) commonly used to stain dsDNA were examined to determine if they could bind the modified proteins. We first tested ethidium bromide and found that the ONE-modified BSA could be moderately stained by the DNA intercalator (Fig. 1c). We also tested an alternative probe, SYBR Green I (SG), which appeared to be much more sensitive than ethidium bromide (Fig. 1d). Of interest, the ONE-modified BSA not only showed a stability against heat denaturation, but also retained its SG-binding potential after the heat treatment (Fig. S2), suggesting that the ONE modification may result in the preferential enrichment of the stably-folded structure in proteins. Furthermore, the oxidative modification of low-density lipoproteins (LDL), generating a number of lipid peroxidation-derived aldehydes including ONE, was accompanied

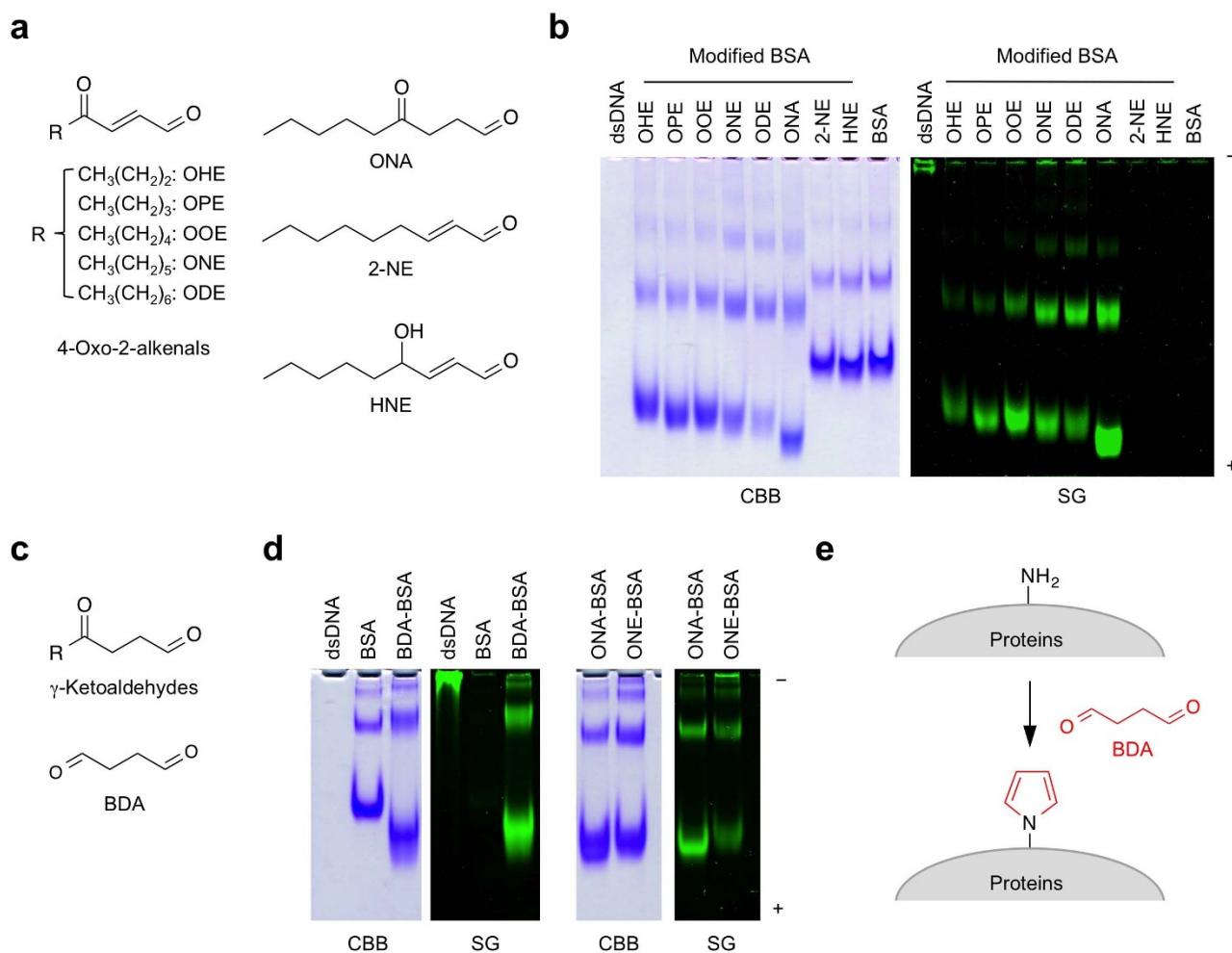


**Figure 2 | Pyrrolated proteins as a target of DNA intercalators.** (a) Chemical structures of 4-oxo-2-alkenals and related aldehydes. Abbreviations: OHE, 4-oxo-2-hexenal; OPE, 4-oxo-2-heptenal; OOE, 4-oxo-2-octenal; OHE, 4-oxo-2-hexenal; ODE, 4-oxo-2-decenal; ONA, 4-oxononanal; 2-NON, 2-nonenal; HNE, 4-hydroxy-2-nonenal. (b) Binding of SG to the modified proteins with 4-oxo-2-alkenals and related aldehydes. (c) General structures of  $\gamma$ -ketoaldehydes and chemical structure of 1,4-butanediol (BDA). (d) Binding of SG to the modified proteins with  $\gamma$ -ketoaldehydes. (e) Formation of a pyrrole derivative upon reaction of primary amines with BDA.

by the increase in the SG-binding potential (Fig. 1e). This result and the previous finding that oxidized LDL is present in the atherosclerotic lesions of all examined animal models and humans<sup>14</sup> suggest the SG-binding proteins could be ubiquitously generated through lipid peroxidation modification of proteins *in vivo*.

To determine the structure essential for the recognition by the DNA intercalators, the aldehydes with chain lengths varying from three to ten carbons were tested. The ONE-modified proteins were very efficiently recognized by SG, whereas the modified proteins with the reactive aldehydes, such as the 2-alkenals, 4-hydroxy-2-nonenal, methylglyoxal, and malondialdehyde, were barely stained (Fig. S3). Of interest, the  $\gamma$ -ketoaldehyde derivatives typically showed a potent activity for the formation of the SG-binding proteins (Fig. 2a, b). The binding studies with ethidium bromide also gave similar results (Figs. S4 and S5). 1,4-Butanedial (BDA), the simplest  $\gamma$ -ketoaldehyde, was identified to be the most efficient source of the SG-binding proteins (Fig. 2c, d). The observations that (i) similar dialdehydes with different chain lengths, such as malondialdehyde and glutaraldehyde, did not generate the SG-binding proteins (Fig. S6), and (ii) the serum albumins, among the tested proteins, upon treatment with BDA were most efficiently stained by SG (Fig. S7) suggest the specificity of the  $\gamma$ -ketoaldehyde-modified serum albumins upon recognition by the DNA intercalator. We therefore speculated that the protein-bound pyrroles, a major product of the  $\gamma$ -ketoaldehyde modification of

proteins (Fig. 2e)<sup>15</sup>, might be, at least in part, involved in their SG-binding potential.

**Enhancement of SG fluorescence by  $\gamma$ -ketoaldehyde-modified proteins.** It has been established that intercalation between base pairs and stabilization of the electrostatic SG/dsDNA complex contributes to the increased SG affinity to dsDNA<sup>16</sup>. In a manner similar to the SG/dsDNA, the fluorescence of SG was dramatically enhanced by the BDA-modified proteins (Fig. 3a, b). A very limited overall alteration in the secondary structure of the protein after treatment with the  $\gamma$ -ketoaldehydes, such as 4-oxo-nonanal and BDA, was observed (Fig. S8). These data support the hypothesis that the protein-bound pyrroles might be involved in the structural and chemical criteria governing the recognition of the modified proteins by the DNA-binding molecules (Fig. 3c).

**Identification of  $N^\epsilon$ -pyrrolylsine as a key adduct.** To characterize the chemical properties of the  $\gamma$ -ketoaldehyde-modified serum albumins as a target of the DNA intercalators, we examined the formation of the pyrrolated adduct(s) in the BDA-modified protein. Because the general methods for the acid hydrolysis of protein (e.g., 6N HCl at 105°C for 24 h) were postulated to decompose the pyrrole structures, the modified proteins were hydrolyzed by 2 N NaOH under an argon atmosphere for 18 h at 120°C. Mainly three products, including two

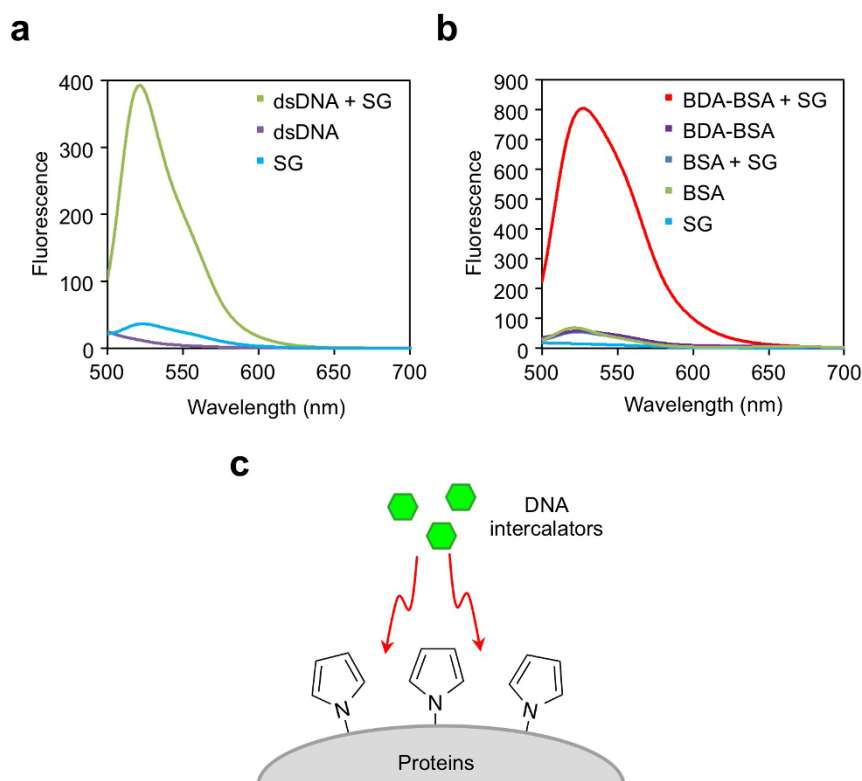


**Figure 3 | Fluorescence spectra of SG free in solution and in complex with dsDNA or BDA-modified BSA.** (a) Fluorescence spectra of SG in complex with dsDNA. dsDNA (1 mg/ml) was incubated with SG (100 nM) in TAE buffer for 30 min. (b) Fluorescence spectra of SG in complex with BDA-modified BSA. BSA or BDA-modified BSA (1 mg/ml) were incubated with SG (500 nM) in TAE buffer for 30 min. (c) A schematic illustration of the binding of DNA intercalators to the pyrroled proteins.

aromatic amino acids (Phe and Trp) and one unknown product (P-1), were detected in the hydrolysate of the BDA-modified protein (Fig. 4a). The LC-MS ( $m/z$  of 197.1 [M + H]<sup>+</sup>) of P-1 was completely identical to those of the expected BDA-lysine adduct (*N*<sup>ε</sup>-pyrrolylsine) (Fig. 4b). The product was also eluted at the same retention time as that of the authentic *N*<sup>ε</sup>-pyrrolylsine prepared by the reaction of L-lysine with BDA. The treatment of BSA with BDA (0–1 mM) in phosphate-buffered saline for 24 h at 37°C resulted in the dose-dependent formation of *N*<sup>ε</sup>-pyrrolylsine (Fig. 4c). In addition, the formation of *N*<sup>ε</sup>-pyrrolylsine in the BDA-modified protein correlated well with the recognition of the protein by SG (Fig. 4d). We further characterized the *N*<sup>ε</sup>-pyrrolylsine formation sites using nano-LC-ESI-Q-TOF MS (Fig. S9, Table S1-1–S1-3) and found that BDA could be incorporated into Lys-4, 12, 106, 127, 180, 187, 204, 211, 221, 224, 239, 261, 273, 280, 377, 388, 413, 431, 439, 465, 471, 474, and 524 (Fig. S10-1–S10-25). It appeared that the formation of *N*<sup>ε</sup>-pyrrolylsine mainly occurred in the IIA and IIIA subdomains. This agrees with the fact that the vast majority of albumin ligands are bound in one or both sites within specialized cavities of these subdomains<sup>17</sup>. The albumin ligands, such as palmitic and myristic acids, indeed inhibited the SG staining of the modified proteins in a dose-dependent manner (Fig. S11). The computational analysis of the BDA-modified BSA showed that the pyrrolation produced a distinctive charge distribution on the protein surface (Fig. S12). In contrast to the native BSA, the surface of the pyrroled BSA became more hydrophobic in domains IIA and IIIA due to the formation of a substantial number of *N*<sup>ε</sup>-pyrrolylsines (Fig. 4e). Thus, although the exact location of the bound SG in the subdomains remains unclear, the pyrroled lysine residues generated in specific subdomains and the narrow fit of SG between the *N*<sup>ε</sup>-pyrrolylsine residues and/or between *N*<sup>ε</sup>-pyrrolylsine and the aromatic amino acid residues may be responsible for the unusual staining of the proteins by the DNA intercalators.

**Pyrroled proteins act as a DNA mimic.** Because pyrrolation is an amino charge-neutralizing reaction, it was speculated that the BDA modification might give rise to the generation of electronegative proteins. An enhanced anodic mobility of the BDA-treated protein compared to the native protein was indeed observed during gel electrophoresis (Fig. 2d). We also evaluated the electronegativity of the BDA-modified proteins by measuring the zeta potential, an electrochemical property determined by the net electrical charge of the molecules. The zeta potential of the native BSA was −12 mV, which is in agreement with the previously reported zeta-potential of ~−10 mV for BSA<sup>18</sup>. The zeta potential of the protein decreased upon BDA modification, in which a zeta-potential as low as −30 mV was observed (Fig. 5a). Thus, the reduction in the zeta potential was consistent with the enhanced anodic mobility of the modified protein observed during the gel electrophoresis.

On the other hand, pyrrole is one of the most used monomers for the preparation of electroconducting polymeric materials. Based on the observation that the BDA modification generated a significant amount of *N*<sup>ε</sup>-pyrrolylsine in the protein, the electric property of the pyrroled protein was investigated. Figure 5b shows the temperature dependence of the conductivity of the native and BDA-modified proteins that could be well described by the Arrhenius relation with a single activation enthalpy for each. As expected, the conductivity of the pyrroled protein was much higher than that of the native protein. The pyrroled protein showed an electrical conductivity of  $2.1 \times 10^{-6} \text{ Scm}^{-1}$  at 324 K. Thus, the introduction of the pyrrole structure in the protein through BDA modification resulted in the formation of an electric semiconductor (Fig. 5c).

**Pyrrolation transforms self-molecules into autoantigens.** To evaluate the biological significance of the protein pyrrolation as a source of DNA mimic proteins, we examined the autoantigenic property of the pyrroled self-proteins. Balb/c mice were

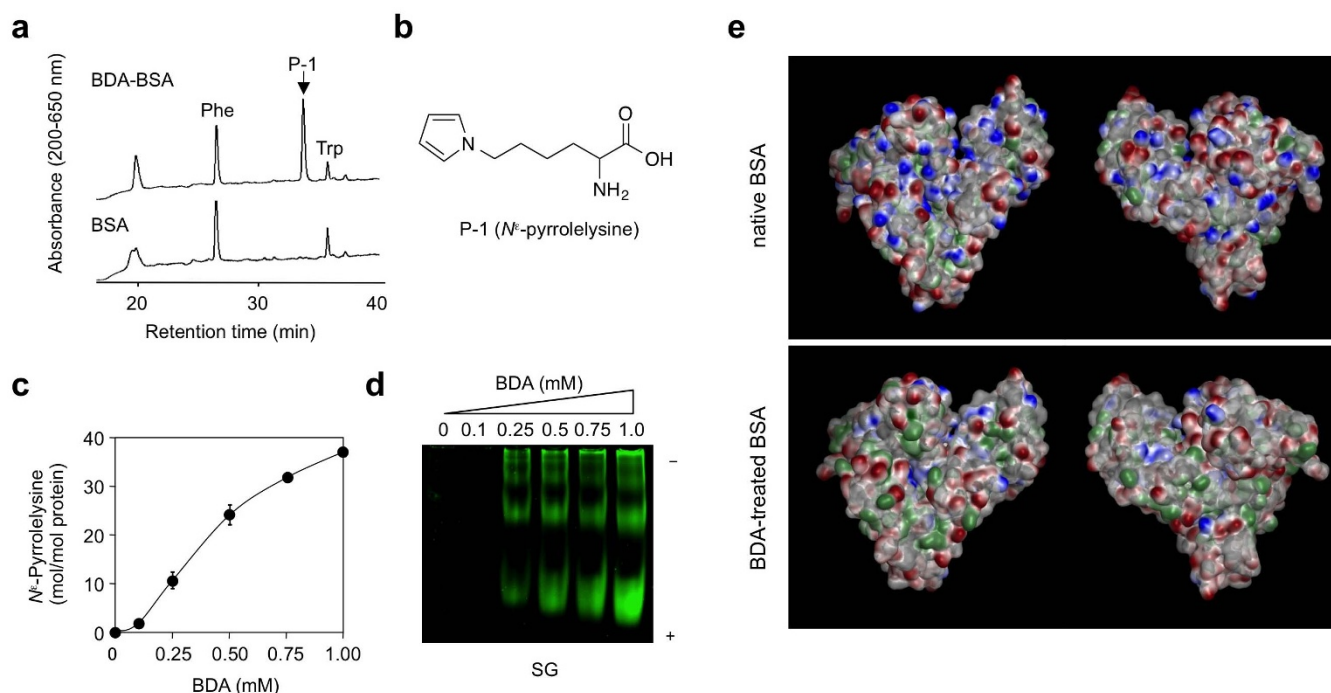


**Figure 4 | Formation of  $N^\epsilon$ -pyrrolysine in the BDA-modified proteins.** (a) HPLC detection of  $N^\epsilon$ -pyrrolysine in the BDA-modified proteins. The BDA-modified protein was prepared by incubating BSA (1.0 mg/ml) with 1 mM BDA in PBS at 37°C for 24 h. The protein samples were hydrolyzed by 2 N NaOH under argon atmosphere for 18 h at 120°C. After the alkaline hydrolysis, the samples were neutralized with hydrochloric acid and analyzed by reverse-phase HPLC. Chromatogram: *upper*, BDA-treated BSA; *lower*, BSA. (b) Chemical structure of  $N^\epsilon$ -pyrrolysine. (c) Measurement of  $N^\epsilon$ -pyrrolysine generated in the BDA-modified proteins. The native and modified BSAs were analyzed by LC-ESI-MS in the selected ion monitoring (SIR) mode followed by alkaline hydrolysis. (d) Binding of SG to the BDA-treated BSA. BSA (1.0 mg/ml) was incubated with BDA (0–1 mM) in 1 ml of PBS at 37°C for 24 h. (e) Changes in electric properties on the molecular surface of both sides of native and BDA-modified BSA. The BDA-modified protein was prepared by incubating BSA (1.0 mg/ml) with 1 mM BDA in PBS at 37°C for 24 h. Panels: *upper*, native BSA; *lower*, BDA-treated BSA. The left and right panels represent the pair of images. The left panels show molecules in the orientation with domain I on the left and further domains arranged counterclockwise, whereas in the right panels, domain I is on the right and the domains are arranged clockwise. Colored residues: red, negative amino acids; blue, positive amino acids; green, hydrophobic amino acids including pyrrolylated lysine.

immunized every two weeks with the BDA-modified mouse serum albumin (MSA) emulsified with complete Freund's adjuvant, and the Ab responses to the DNA and pyrrolylated BSA were examined. The Ab titers to both antigens were enhanced by the immunization with the pyrrolylated MSA (Fig. 6a). We then isolated the hybridoma clones, producing mAbs specific for the DNA and/or pyrrolylated proteins, from the mice and characterized their specificity in detail. Spleen cells from the balb/c mice immunized with the pyrrolylated MSA were fused with P3/U1 murine myeloma cells and, after screening based on a specific binding to the pyrrolylated proteins, we established one hybridoma clone, PSB, producing the mAb specific for the pyrrolylated protein. The mAb PSB established from the mice immunized with the pyrrolylated protein was found to be IgM. Of interest, the specificity study showed that the mAb cross-reacted with multiple antigens, including dsDNA and aldehyde-modified proteins (Fig. 6b).

**Pyrrolylated proteins as a molecular target of autoimmunity.** The observations that the pyrrolylated proteins showed a significant cross-reactivity with the SLE sera and the anti-DNA mAb (Fig. 7a) suggested that the production of specific antibodies against the pyrrolylated proteins might be accelerated in autoimmune diseases, such as SLE. Hence, we evaluated the Ab titers to the pyrrolylated proteins in the SLE-prone MRL-*lpr* mice. When the age-dependent change in the Ab titers was measured in the sera from the MRL-*lpr* mice and control MRL-MpJ mice, only the MRL-*lpr* mice displayed a spontaneous age-dependent elevation of the IgG and IgM responses to both DNA and the pyrrolylated proteins (Fig. 7b). We established

the IgM mAb PSL from the MRL-*lpr* mice, which showed specificities toward multiple antigens, including dsDNA and the pyrrolylated proteins (Fig. S13). Of interest, the mAb PSL mainly cross-reacted with the modified proteins that showed binding potentials with SG.

Glomerulonephritis is a major cause of morbidity and mortality in patients with SLE. The deposition of autoAbs in the glomeruli plays a key role in the development of lupus nephritis. We assessed the specificity of the Abs that was deposited in glomeruli of the MRL-MpJ and MRL-*lpr* mice and observed that the titers of the anti-pyrrolylated proteins Abs were significantly higher in the MRL-*lpr* mice than in the MRL-MpJ mice (Fig. 7c).

We also evaluated the presence of the antibodies against pyrrolylated proteins in autoimmune disease patients, such as SLE (n=26) and IgA nephropathy (n=20), and in the healthy controls (n=5). The ELISA measurement showed that the serum IgG titers to the DNA and pyrrolylated proteins significantly varied among patients with SLE and IgA nephropathy. The levels of the anti-DNA titers in the SLE patients were notably higher than those in the healthy individuals and IgA nephropathy patients (Fig. 7d, left). The SLE patients also exhibited prominent increases in the Ab titers to the pyrrolylated proteins (Fig. 7d, right). The pull-down assay also confirmed the enhanced production of IgG and IgM that recognize the pyrrolylated proteins in the SLE patients (Fig. S14).

**Presence of pyrrolylated proteins *in vivo*.** Finally, to gain an insight into the formation of DNA mimic proteins *in vivo*, we established a highly sensitive and specific method for the measurement of  $N^\epsilon$ -

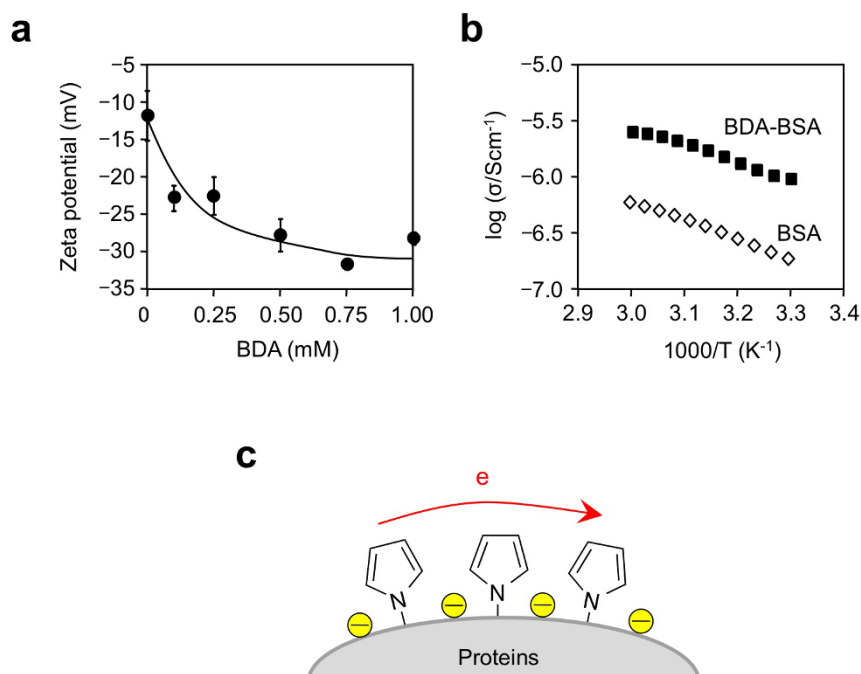


**Figure 5 | Pyrrolated proteins act as a DNA mimic.** (a) Zeta potential of the BDA-treated proteins. BSA (1.0 mg/ml) was incubated with BDA (0–1 mM) in 10 mM sodium phosphate buffer (pH 7.4) for 24 h at 37°C. (b) Temperature dependence of ionic conductivity for native and BDA-treated proteins. The BDA-modified protein was prepared by incubating 10 mg BSA with 10 mM BDA in 2.0 ml of distilled water at 37°C for 24 h. Native and BDA-treated proteins were dialyzed against distilled water, lyophilized, and subjected to the ionic conductivity measurement. (c) A schematic illustration of the electron transfer in pyrrolated proteins.

pyrrolylsine using LC-ESI-MS/MS coupled with a stable isotope dilution method (Fig. 8a, Fig. S15). When the alkaline hydrolysates of the sera from normal humans and balb/c mice were analyzed, the pyrrolylsine was detected in all tested samples (Fig. 8b, c). Subsequently, we measured *N*<sup>ε</sup>-pyrrolylsine in the immune complex deposits in the kidneys from the SLE-prone MRL-*lpr* and control MRL-MpJ mice and found that, while there was no difference in the serum *N*<sup>ε</sup>-pyrrolylsine levels between the MRL-*lpr* and MRL-MpJ mice (Fig. S16), the pyrrolylsine was accumulated more in the SLE mice than in the control mice (Fig. 8d). The result is

consistent with the observation that the levels of Abs against the pyrrolylsine in the immune complex deposits were higher in the MRL-*lpr* mice than in the control mice (Fig. 7c). These data provided direct evidence, for the first time, that the pyrrolylation of proteins, generating *N*<sup>ε</sup>-pyrrolylsine, occurs *in vivo*.

## Discussion

In the present study, we gained a deeper insight into what constitutes the multi-specificity of the anti-DNA autoAbs. A remarkable finding is that the DNA-binding molecules, such as SG, showed the ability to

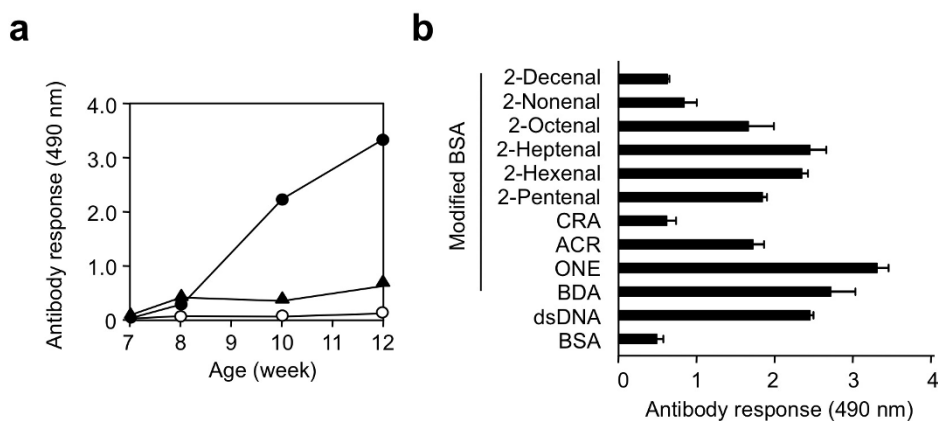


**Figure 6 | Pyrrolation transforms self-molecules into autoantigens.** (a) Elevation of immune response to pyrrolated proteins and dsDNA in the balb/c mice immunized with the pyrrolated MSA. Female balb/c mice were immunized with complete Freund adjuvant and 50 μg of the BDA-modified MSA, and then boosted every 2 weeks with incomplete Freund adjuvant by emulsifying and intraperitoneal injection. The Ab titers were determined by ELISA using the BSA, BDA-modified BSA (pyrrolated BSA), and DNA as the absorbed antigens. Symbols: *open circle*, anti-BSA titer; *closed circle*, anti-pyrrolated BSA titer; *closed triangle*, anti-DNA titer. (b) Immunoreactivity of the anti-pyrrolated proteins mAb PSB established from the balb/c mice immunized with the pyrrolated MSA. The coating antigen was prepared by incubating BSA (1 mg/ml) with 1 mM aldehyde in 1 ml of PBS for 24 h at 37°C. Five microgram of antigen was coated per well on polystyrene plates and antibody binding detected. CRA, crotonaldehyde, ACR, acrolein; ONE, 4-oxo-2-nonenal; BDA, 1,4-butanediol.

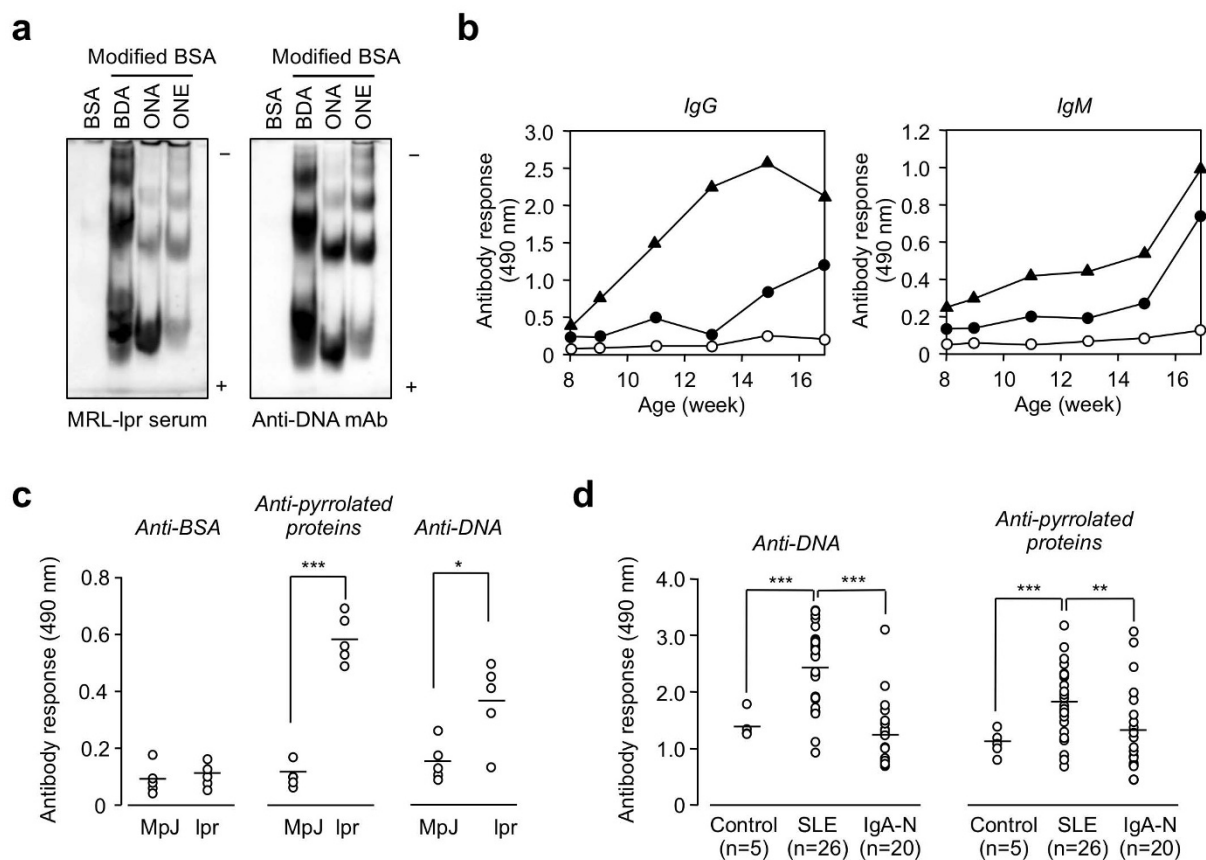


**Figure 7 | Pyrrolated proteins as a molecular target of autoimmunity.** (a) Recognition of the pyrrolated proteins by anti-DNA autoAbs. *Left*, immunoblot analysis of the modified proteins using the sera from MRL-*lpr* mice. *Right*, immunoblot analysis of the modified proteins using the anti-DNA monoclonal IgG DSO established from female MRL-*lpr* mice. (b) Age-dependent elevation of antibody response to both DNA and pyrrolated proteins in SLE-prone MRL-*lpr* mice ( $n=5$ ) compared to those in the wild-type MRL-MpJ mice ( $n=5$ ). *Left*, IgG response. *Right*, IgM response. The Ab titers were determined by ELISA using BSA, BDA-treated BSA (pyrrolated BSA), and dsDNA as the absorbed antigens. Symbols: *open circle*, anti-BSA titer; *closed circle*, anti-pyrrolated BSA titer; *closed triangle*, anti-DNA titer. (c) Immunoreactivity of Abs eluted from the kidneys of the MRL-MpJ mice and MRL-*lpr* mice. Affinity of the Abs was determined by a direct antigen ELISA using BSA (*left*), pyrrolated BSA (*middle*), and dsDNA (*right*) as the absorbed antigens. The means were tested for statistical significance by Welch's test analysis. Statistically significant differences between the MRL-MpJ and MRL-*lpr* mice are indicated by asterisks (\*,  $P < 0.05$ ; \*\*\*,  $P < 0.005$ ). (d) Elevation of immune response to dsDNA (*left panel*) and pyrrolated proteins (*right panel*) in autoimmune diseases. The plasma samples were prepared from 5 healthy individuals, 20 patients with IgA nephropathy (IgA-N), and 26 patients with SLE. The levels of the IgG Abs against the dsDNA and pyrrolated proteins in the plasma samples were measured by ELISA using calf-thymus dsDNA and pyrrolated BSA, respectively, as the coating antigens. The means were tested for statistical significance by Welch's test analysis. Statistically significant differences between control and SLE and between SLE and IgA-N are indicated by asterisks (\*\*,  $P < 0.01$ ; \*\*\*,  $P < 0.005$ ).

bind the proteins that could be recognized by the anti-DNA autoAbs. SG is an asymmetrical cyanine DNA-binding dye that provides an opportunity for increasing the sensitivity of the nucleic acid detection when used in conjunction with gel electrophoresis. SG is not fluorescent unless it is bound to dsDNA. The alterations in the fluorescence emission of the free and DNA-bound SG and the underlying mechanisms depend on the structure and binding mode of SG. An analysis of the SG/dsDNA association has revealed that the dye forms the following three different interactions with dsDNA: intercalation between base pairs, electrostatic interaction, and extended contact with the groove of dsDNA<sup>16</sup>. It had been generally believed that SG is not able to bind non-nucleic acid biomolecules like proteins. However, the present study revealed that it could stain proteins when modified with  $\gamma$ -ketoaldehydes. To the best of our knowledge, this is the first report describing the recognition of non-nucleic acid biomolecules by the DNA intercalating agent.

Based on the fact that the  $\gamma$ -ketoaldehydes primarily react with the lysine residues of proteins to form pyrrole derivatives, the protein-bound pyrroles were speculated to be an unrecognized target of the DNA-binding molecules. The five-membered heteroaromatic pyrrole ring is planar and electron rich, highly susceptible to electro-

philic attack, capable of oxidation and able to participate in both  $\pi$ - $\pi$  stacking and hydrogen-bonding interactions. Members of this important class of heterocyclic compounds also display a variety of pharmacological properties including antibacterial, antiviral, anti-inflammatory, anticancer, and antioxidant activities. In addition, the pyrrole framework is a ubiquitous structural motif found in a wide range of biologically active natural products and pharmaceutically active agents. The detailed mechanism for the unusual binding of SG to the pyrrolated proteins still remains unknown. However, the structural features of the DNA intercalator might, at least in part, be involved. The SG molecule contains phenylquinilinium and benzothiazole aromatic systems and dimethylaminopropyl and propyl elongated chains. Each of these structural elements contributes to the energy of the SG/dsDNA complex formation. The aromatic rings of SG intercalate into dsDNA, an interaction that is energetically favorable<sup>19</sup>. In a manner similar to the intercalation into dsDNA, the narrow fit of the aromatic group between the  $N^{\epsilon}$ -pyrrolylsine residues and/or between  $N^{\epsilon}$ -pyrrolylsine and the aromatic amino acid residues coupled with van der Waals interactions with the pyrrole ring may significantly dampen the internal motion of SG. An additional SG molecular rigidity may also come from the electrostatic

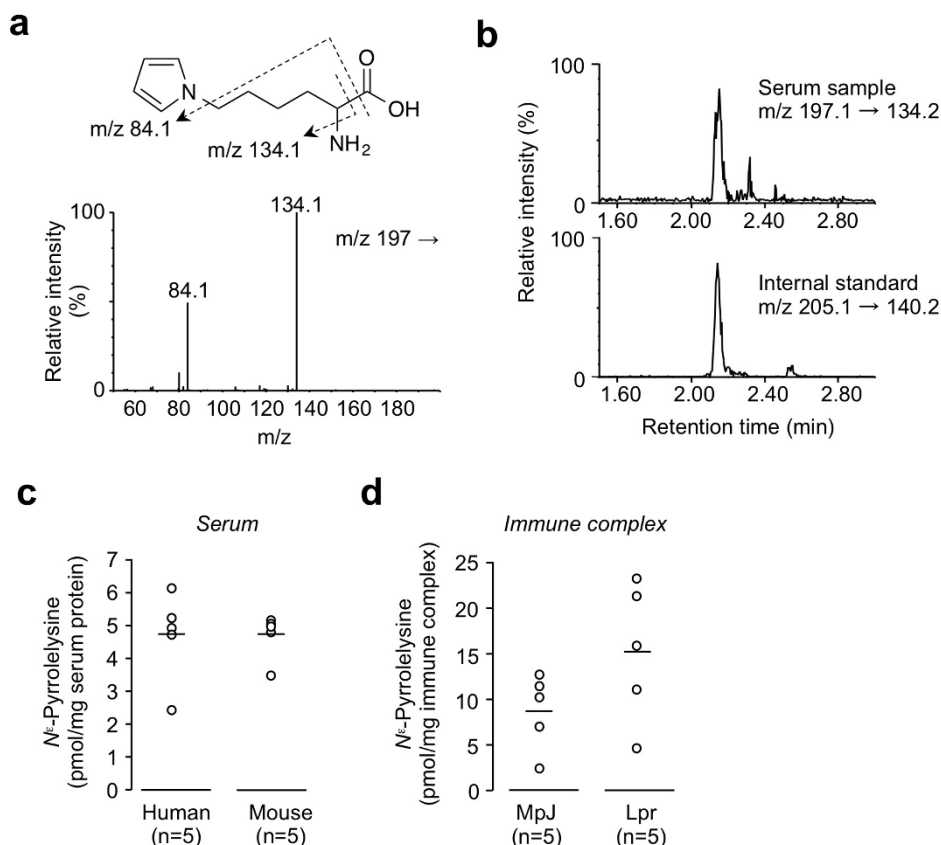


**Figure 8 | Presence of  $N^\epsilon$ -pyrrolylysine *in vivo*.** (a) Collision-induced dissociation of the  $[M+H]^+$  of  $N^\epsilon$ -pyrrolylysine at  $m/z$  197 at a collision energy of 25 V. (b) LC-ESI-MS/MS analysis of authentic isotope-labeled [ $^{13}C_6$ ,  $^{15}N_2$ ]  $N^\epsilon$ -pyrrolylysine (lower) and  $N^\epsilon$ -pyrrolylysine in the hydrolysate of normal human serum (upper). The ion current tracings with SRM are shown. (c) LC-ESI-MS/MS analysis of  $N^\epsilon$ -pyrrolylysine in the hydrolysates of sera from normal human ( $n=5$ ) and male balb/c mice (15w,  $n=5$ ). (d) LC-ESI-MS/MS analysis of  $N^\epsilon$ -pyrrolylysine in the immune complex deposits in the kidneys from the SLE-prone MRL-*lpr* and control MRL-MpJ mice.

interactions between SG and the pyrrolylated proteins; the SG/pyrrolylated protein complex can be stabilized by a charge-charge interaction formed by the positively charged thiazole group and carboxylic acids from the protein side-chains. Thus, the intercalation and columbic interaction may effectively immobilize the quinilinium-thiazole system in a favorable conformational state, which is characterized by a dramatic enhancement of the SG fluorescence.

It is also noted that the modification of proteins by  $\gamma$ -ketoaldehydes is associated with an increase in the net negative charges of the proteins due to the modification of the lysine residues and formation of amino charge-neutralized structures, such as pyrrole. This may give rise to the structural similarity to the dsDNA backbone, which is composed of negatively charged phosphate groups. Indeed, the binding to dsDNA is one example of the potential cross-reactivities with flexible phosphodiester polymers, such as RNA, teichoic acid, or other molecules whose distribution of phosphates or similar negatively charged epitopes conform with the available contacts in the anti-DNA combining site<sup>20</sup>. In addition, the pyrrolylation by BDA produced an electronic semiconductor protein (Fig. 5). It may be likely that, although the detailed mechanisms underlying these electronic properties of the pyrrolylated proteins remain unknown, some of the electron orbitals belonging to the pyrrole overlap with each other along the long axis of the protein. These so-called stacking interactions indeed underlie many of the one-dimensional molecular conductors. The lysine-bound pyrroles in proteins may therefore be ideal for electron transfer. Based on the fact that dsDNA transports an electrical current as efficiently as a good semiconductor<sup>21</sup>, the  $\gamma$ -ketoaldehyde-modified proteins may potentially constitute an electrical mimic to the dsDNA. These electronegativity and electronic

properties may be closely associated with the fact that the anti-DNA autoAbs often bind to non-nucleic acid biomolecules.

This study proved for the first time that the pyrrolylation transforms self-molecules into autoantigens. The immunization of balb/c mice with the pyrrolylated self-molecule (MSA) indeed accelerated the production of autoAbs (Fig. 6). The spontaneous age-dependent increase in the IgG and IgM titers to the dsDNA and pyrrolylated proteins was also observed in the SLE-prone MRL-*lpr* mice (Fig. 7). Moreover, we measured the Ab titer against the BDA-modified proteins, along with the Ab titer against dsDNA, in the sera from the SLE patients and observed that the patients exhibited prominent increases in the Ab titers to both antigens. These data emphasize the relevance of the pyrrolylated proteins for the anti-DNA response in SLE. Although the potential role in pathogenesis needs to be further explored, protein pyrrolylation may not simply be an associated side effect of the disease progression, but a possible etiology of SLE and other autoimmune diseases.

Using the LC-ESI-MS/MS technique, we successfully detected  $N^\epsilon$ -pyrrolylysine in the protein hydrolysates of human and mouse sera (Fig. 8). The *in vivo* origin of lysine pyrrolylation currently remains unknown. As BDA is not physiologic, some other endogenous molecules are suggested to be involved in the formation of  $N^\epsilon$ -pyrrolylysine. However, the conversion of the primary amino groups into pyrrole derivatives has been shown to occur upon modification of the lysine residues of proteins with various lipid peroxidation-derived aldehydes, such as 4-hydroxy-2-nonenal<sup>22,23</sup>, 4,5-epoxy-2-alkenals<sup>24</sup>, and 4-oxo-2-alkenals<sup>25</sup>. Levuglandin E2, a metabolite of arachidonic acid, also adds to protein amino groups, presumably as pyrrole derivatives<sup>26</sup>. Moreover, the unsaturated epoxyoxo fatty acids





have also been shown to generate pyrrole derivatives that incorporate the  $\epsilon$ -amino group of lysine residues<sup>27</sup>. The formation of different types of pyrrole derivatives produced in these reactions has indeed been observed in a variety of diseases, including atherosclerosis<sup>28</sup>. Furthermore, the increased carboxyalkylpyrrole immunoreactivity was detected in the plasma from patients with renal failure and atherosclerosis when compared to healthy volunteers<sup>29</sup>. Thus, a physiologically relevant metabolite of fatty acids is likely to be involved in the formation of  $N^\epsilon$ -pyrrolylsine. To test this hypothesis, studies are now underway to identify the putative oxidized fatty acid metabolites.

In conclusion, we identified pyrrolation as a key modification reaction of proteins involved in the recognition by the DNA-binding molecules, such as the anti-DNA autoantibodies and DNA intercalators. Strikingly, the pyrrolated proteins showed electronegativity and electronic properties on the proteins that potentially constitute an electrical mimic to the DNA. They present *in vivo* and indeed triggered an autoimmune response. Future studies need to evaluate the contribution of this newly established covalent protein modification in the pathogenesis of human diseases, including autoimmune disease.

## Methods

**Materials.** The DNA intercalators, ethidium bromide and SYBR Green I (SG), were obtained from Nacalai Tesque and Invitrogen, respectively. Single-stranded and double-stranded DNA, dGdT, dGdC, and dGdA were obtained from Sigma. The anti-DNA monoclonal antibody (mAb) DSO was prepared from the MRL-*lpr* mice<sup>13</sup>. The stock solutions of HNE were prepared by the acid-treatment (1 mM HCl) of HNE dimethylacetal, which was synthesized according to the procedure of De Montarby et al.<sup>30</sup> ONE was synthesized from 2-pentylfuran according to the procedure of Sun et al.<sup>31</sup> The other aldehydes were purchased from the Cayman Chemical Co. (Ann Arbor, MI). The horseradish peroxidase (HRP)-linked anti-rabbit IgG immunoglobulin, HRP-NeutrAvidin, and ECL (enhanced chemiluminescence) Western blotting detection reagents were obtained from GE Healthcare.

**Animals.** Female and male balb/c mice, female MRL-MpJ mice, and female MRL-*lpr* mice were purchased from Japan SLC (Hamamatsu, Japan). The care and use of all animals were performed in accordance with prescribed national guidelines, and the Animal Care and Use Committee of Nagoya University granted ethical approval for the study.

**Plasma samples.** Plasma samples were obtained from 5 healthy individuals and 20 patients with IgA nephropathy and 26 patients with SLE who underwent diagnostic evaluation at the Nagoya University Hospital (Nagoya, Japan). The antibody (Ab) titers against DNA and pyrrolated proteins in the plasma samples were measured by ELISA using calf-thymus DNA and BDA-modified BSA, respectively, as the coating antigens. This study was approved by the Ethical Committee of the Nagoya University School of Medicine.

**Staining of proteins by DNA intercalators.** Electrophoresis was performed in a nondenaturing polyacrylamide gel (8% acrylamide) in  $2\times$ TAE buffer (80 mM Tris-acetate, 2 mM EDTA, pH 8.0). Tris-glycine, pH 8.4, was used as the running buffer. Thirty  $\mu$ l of 0.5 mg/ml protein was mixed with 6  $\mu$ l of 6 $\times$  loading buffer (0.03% bromophenol blue, 10 mM TrisHCl, pH 7.6, 60 mM EDTA, 60% glycerol) and electrophoresed in the gel at 100 V. After electrophoresis, the gels were rinsed in ultrapure water and stained with Coomassie Brilliant Blue or 2.5 mg/ml of SG dissolved in TAE buffer for 30 min. Fluorescence scanning of the gels was carried out using a Typhoon 9200 fluorescence gel scanner (GE Healthcare). For staining with ethidium bromide, electrophoresis was performed in a 1% agarose gel in  $1\times$ TAE buffer. After electrophoresis, the gels were stained with 2.5 mg/ml of ethidium bromide dissolved in TAE buffer for 30 min, and fluorescence scanning of the gels was carried out using a gel imaging system (AE-6932 GXCF, ATTO, Tokyo, Japan).

**Zeta potential.** BSA (1.0 mg/ml) was incubated with BDA (0–1 mM) in 10 mM sodium phosphate buffer (pH 7.4) at 37°C. The zeta potential measurement was performed using a zeta potential analyzer (Zetasizer Nano ZS, Malvern).

**Electrical conductivity.** The samples were prepared by incubating BSA (1 mg/ml) with or without 1 mM BDA at 37°C for 24 h in deionized distilled water. After incubation, the reaction mixtures were dialyzed against the deionized distilled water, freeze dried, and then their conductivities were measured. The electrical conductivity was measured by a complex-impedance gain-phase analyzer (Solartron model 1260; Schlumberger) in the frequency range from 1 Hz to 1 MHz. The protein samples were thoroughly dried under vacuum for 24 h prior to the measurements.

**Modeling analysis.**  $N^\epsilon$ -Pyrrolylsine was generated and energy-minimized using the Molecular Operating Environment (MOE) (Chemical Computing Group, Montreal, Canada). The positions of the  $N^\epsilon$ -pyrrolylsine were adjusted using the MOE. The surface electric potential was calculated from the coordinate of the BSA structure (PDB: 4F5S) using the MOE.

**Fluorescence measurements.** Fluorescence spectra of free SG and SG in complex with dsDNA or BDA-modified BSA were measured on a FP-6500 (JASCO, Japan) spectrofluorimeter at room temperature. SG was excited at 485 nm and the fluorescence monitored over the wavelength range of 490 to 700 nm. A 0.3 cm path-length quartz cell was used.

**CD spectroscopy.** The CD spectra were measured at 20°C using a J-820 spectropolarimeter (JASCO, Japan) and a 1-mm cell in PBS without EDTA at a protein concentration of 0.15 mg/ml.

**Reaction of L-lysine with BDA.** To identify a putative BDA-lysine adduct detected in the LC-MS analysis of the hydrolysates of the BDA-modified proteins, products obtained from the reaction of L-lysine with BDA were characterized. The reaction mixture contained 10 mg/ml L-lysine and 10 mM BDA in PBS. After incubation for 24 h at 37°C, the reaction mixtures were analyzed by a reversed-phase HPLC using a Develosil C30-UG-5 (4.6  $\times$  250 mm, Nomura Chemical, Japan) at the flow rate of 0.8 ml/min. A discontinuous gradient was used by solvent A ( $H_2O$  containing 0.1% trifluoroacetic acid) with solvent B (acetonitrile containing 0.1% trifluoroacetic acid) as follows: 5% B at 0–5 min, 30% B at 40 min, 100% B at 40.1 min. The elution profiles were monitored by the absorbance at 200–650 nm. The reaction provided two major products, which were suggested to be the  $N^\epsilon$ -pyrrolated and  $N^\epsilon$ -pyrrolated lysines based on their fragmentation patterns in the LC-MS analysis. The product corresponding to  $N^\epsilon$ -pyrrolylsine was isolated (Fig. S17) and characterized by high resolution MS, and  $^1H$ - and  $^{13}C$ -NMR (Fig. S18–20). High resolution MS, m/z of 197.1283 [M+H]<sup>+</sup>,  $C_{10}H_{17}N_2O_2$ ; NMR,  $^1H$ -NMR ( $D_2O$ )  $\delta$ H 1.29–1.454 (2H, m),  $\delta$ H 1.81–1.95 (4H, m),  $\delta$ H 3.81 (1H, dd),  $\delta$ H 3.99 (2H, dd),  $\delta$ H 6.21 (2H, d),  $\delta$ H 6.87 (2H, s);  $\delta$ C 21.55, 29.79, 30.31, 48.44, 48.47, 54.22, 107.11, 121.40, 174.01. The LC-MS was measured by an ACQUITY TQD system (Waters) equipped with an ESI probe and interfaced with a UPLC system (Waters). The sample injection volumes of 10  $\mu$ l each were separated on a Waters BEH C18 1.7  $\mu$ m column (5 mm  $\times$  2.1 mm) at the flow rate of 0.3 ml/min. A discontinuous gradient was used by solvent A ( $H_2O$  containing 0.1% formic acid) with solvent B (acetonitrile containing 0.1% formic acid) as follows: 5% B at 0 min, 50% B at 10 min, 95% B at 10.1 min. The mass spectrometric analyses were performed on-line using ESI-MS in the positive ion mode (cone potential of 30 eV). High resolution MS was performed by a Mariner ESI-TOF-MS (ABI). The NMR analyses were performed by a Bruker AVANCE 400 (400 MHz) instrument.

**HPLC analysis of  $N^\epsilon$ -pyrrolylsine in the BDA-modified protein.** The BDA-modified protein was prepared by incubating BSA (1.0 mg/ml) with 1 mM BDA in PBS at 37°C for 24 h. For the detection of the BDA-amino acid adducts, the samples (400  $\mu$ l) were delipidated by the addition of 1.25 vol chloroform-methanol (1 : 4, v/v). Tubes were agitated on a vortex mixer and centrifuged at 5,000 rpm for 10 min. An interphase formed, and the fluid above was removed. Methanol (400  $\mu$ l) was added to the samples, then centrifuged at 5,000 rpm for 10 min. The clear organic fluid was removed and the pellet dried under argon. The samples were suspended in  $H_2O$  (50  $\mu$ l) and mixed with 400  $\mu$ l of 2 N NaOH and hydrolyzed by heating under argon for 18 h at 120°C<sup>32</sup>. The resulting solution was neutralized with hydrochloric acid. The samples were analyzed by a reversed-phase HPLC using a Develosil C30-UG-5 (4.6  $\times$  250 mm, Nomura Chemical, Japan) at the flow rate of 0.8 ml/min. A discontinuous gradient was used by solvent A ( $H_2O$  containing 0.1% trifluoroacetic acid) with solvent B (acetonitrile containing 0.1% trifluoroacetic acid) as follows: 5% B at 0–5 min, 30% B at 40 min, 100% B at 40.1 min. The elution profiles were monitored by absorbance at 200–650 nm.

**Nano-LC-ESI-Q-TOF-MS/MS analysis of BDA-modified proteins.** The BDA-modified protein was prepared by incubating BSA (1.0 mg/ml) with 1 mM BDA in PBS at 37°C for 24 h. The protein was proteolyzed with sequence grade modified trypsin (Promega) in 50 mM  $NH_4HCO_3$  buffer in the presence of 0.01% Protease MAX surfactant (Promega) for 3 h at 37°C. The samples were dissolved in 2% acetonitrile in 0.1% trifluoroacetic acid, and subjected to a mass spectrometry analysis. Mass spectrometry was performed using a Triple TOF™ 5600 (AB SCIEX), a hybrid triple quadrupole time-of-flight mass spectrometer equipped with an ESI source, and the mass range was set at m/z 100–1250. The conditions of the MS/MS detector were as follows: ion spray voltage, 2300 V; ion source gas1, 20 psi; interface heater temperature 150°C; curtain gas 20 psi. Nitrogen was used as the nebulizer and auxiliary gas.

**LC-ESI-MS/MS analysis of  $N^\epsilon$ -pyrrolylsine.** Mass spectrometric analyses were performed using an ACQUITY TQD system (Waters) equipped with an ESI probe and interfaced with a UPLC system (Waters). The sample injection volumes of 10  $\mu$ l each were separated on a Develosil HB C30-UG-3 (100 mm  $\times$  2.0 mm, Nomura Chemical, Japan) at the flow rate of 0.3 ml/min. A discontinuous gradient was used by solvent A ( $H_2O$  containing 0.1% formic acid) with solvent B (acetonitrile containing 0.1% formic acid) as follows: 5% B at 0 min, 95% B at 8 min, 95%. Mass spectrometric analyses were performed on line using ESI-MS/MS in the positive ion mode along with the MRM mode (cone potential 25 eV/collision energy 15 eV). The monitored



MRM transitions monitored were as follows: [U-<sup>13</sup>C<sub>6</sub>, <sup>15</sup>N<sub>2</sub>] N<sup>ε</sup>-pyrrolylysine, *m/z* 197.1→134.1; N<sup>ε</sup>-pyrrolylysine, *m/z* 205.1→140.1. The amount of the N<sup>ε</sup>-pyrrolylysine adduct was quantified by the ratio of the peak area of the target adducts and of the reduced N<sup>ε</sup>-pyrrolylysine-stable isotope.

For the LC-ESI-MS/MS analysis of N<sup>ε</sup>-pyrrolylysine, the protein samples were suspended in H<sub>2</sub>O (400 μl). The samples were delipidated by the addition of 1.25 vol chloroform-methanol (1:4, v/v). The tubes were agitated on a vortex mixer and centrifuged at 5,000 rpm for 10 min. An interphase formed, and the fluid above was removed. Methanol (400 μl) was added to the samples, then centrifuged at 5,000 rpm for 10 min. The clear organic fluid was removed and the pellet dried under argon. The proteins were suspended in H<sub>2</sub>O (50 μl) and mixed with 400 μl of 2 N NaOH, then hydrolyzed by heating under argon for 18 h at 120°C. The resulting solution was neutralized with hydrochloric acid. The internal standard, reduced [U-<sup>13</sup>C<sub>6</sub>, <sup>15</sup>N<sub>2</sub>] N<sup>ε</sup>-pyrrolylysine, was added to the samples prior to the digestion. After the digestion, the samples were partially separated with Oasis hydrophilic-lipophilic balance (HLB) cartridges (Waters). After the sample loading, the HLB cartridges were washed with 2 ml of H<sub>2</sub>O, and N<sup>ε</sup>-pyrrolylysine was eluted with 2 ml of 20% acetonitrile. The samples were then dried, and dissolved in H<sub>2</sub>O, and subjected to an LC-ESI-MS/MS analysis.

**ELISA.** A 100-μl aliquot of the antigen solution was added to each well of a 96-well microtiter plate and incubated for 20 h at 4°C. The antigen solution was then removed, and the plate was washed with PBS containing 0.5% Tween 20 (PBS/Tween). Each well was incubated with 200 μl of 4% Blockace (Yukijirushi, Sapporo, Japan) in PBS/Tween for 60 min at 37°C to block the unsaturated plastic surface. The plate was then washed three times with PBS/Tween. A 100-μl aliquot of a 10<sup>2</sup> × dilution of serum was added to each well and incubated for 2 h at 37°C. After discarding the supernatants and washing three times with PBS/Tween, 100 μl of a 5 × 10<sup>3</sup> dilution of goat anti-mouse IgG conjugated to horseradish peroxidase in PBS/Tween was added. After incubation for 1 h at 37°C, the supernatant was discarded, and the plates were washed three times with PBS/Tween. The enzyme-linked Ab bound to the well was revealed by adding 100 μl/well of 1,2-phenylenediamine (0.5 mg/ml) in a 0.1 M citrate/phosphate buffer (pH 5.5) containing 0.003% hydrogen peroxide. The reaction was terminated by the addition of 2 M sulfuric acid (50 μl/well), and the absorbance at 492 nm was read using a micro-ELISA plate reader.

**Western blot analysis.** BSA (1 mg/ml) was incubated with ONE (0–5 mM) in PBS for 24 h at 37°C. The protein samples were electrophoresed through a 10% polyacrylamide gel. After electrophoresis, the gel was transblotted onto a polyvinylidene difluoride (PVDF) membrane (GE Healthcare), incubated with Blockace for blocking, washed, and then incubated with a primary Ab. This procedure was followed by the addition of horseradish peroxidase conjugated to the goat anti-rabbit IgG immunoglobulin and ECL reagents. The bands were visualized using a Light-Capture II (ATTO, Tokyo, Japan).

**Preparation of mAbs.** Spleen cells from the SLE-prone MRL-*lpr* mice were fused with P3/U1 murine myeloma cells and cultured in HAT (hypoxanthine/aminopterin/thymidine) selection medium. The culture supernatants of the hybridoma were screened using an ELISA, employing pairs of wells in the microtiter plates on which were absorbed BDA-treated BSA as antigens (5 μg of protein per well). After incubation with 100 μl of the hybridoma supernatants, and with intervening washes with PBS/Tween, the wells were incubated with horseradish peroxidase goat anti-mouse IgG in PBS/Tween, followed by a substrate solution containing 100 μl/well of 1,2-phenylenediamine (0.5 mg/ml) in a 0.1 M citrate/phosphate buffer (pH 5.5) containing 0.003% hydrogen peroxide. Hybridoma cells, corresponding to the supernatants that were positive on the BDA-modified BSA and the negative on native BSA, were then cloned by limited dilution. After repeated screenings, one clone PSL showing the most distinctive recognition of the BDA-modified BSA was obtained.

The mAbs were also prepared from Balb/c mice immunized with BDA-modified MSA. The immunogen was prepared by incubating MSA (1.0 mg/ml) with 1 mM BDA in PBS (pH 7.4) at 37°C for 24 h. We immunized the female Balb/c mice on week 7 with complete Freund adjuvant and 0.5 mg immunogen (BDA-modified MSA) and boosted on weeks 9 and 11 with incomplete Freund adjuvant, by emulsifying and intraperitoneal injection. The mAbs were prepared from the immunized mice following the same protocol as for the SLE-prone mice.

**Antibody elution study.** The kidneys were thawed, minced, and homogenized in a high-speed blender for 1 min in 4 volumes of cold PBS, and then repeatedly washed in PBS. The washed homogenates were then incubated with 1 ml glycine-HCl buffer (20 mM, pH 3.0) at room temperature for 10 min, centrifuged at 1,500 rpm, and the pH of the supernatant adjusted to pH 7.4. The eluates were dialysed overnight against PBS at 4°C. The samples were assessed for anti-BSA, anti-DNA, and anti-pyrrolylated proteins titers by ELISA and for the LC-ESI-MS/MS measurement of N<sup>ε</sup>-pyrrolylysine.

**Pull-down assay.** The human sera obtained from healthy individuals and SLE patients were preincubated with magnetic beads coated with BSA to preclude the nonspecific binding to beads and/or native BSA for 1 h at room temperature. After preclearing, the supernatants were incubated with magnetic beads coated with BDA-treated BSA for 1 h at room temperature. The beads were then washed three times

with PBS/Tween and bound proteins were eluted into SDS sample buffer by boiling for 5 min and subjected to SDS-PAGE followed by immunoblot analysis.

- Moellering, R. E. & Cravatt, B. F. Functional lysine modification by an intrinsically reactive primary glycolytic metabolite. *Science* **341**, 549–553 (2013).
- Uchida, K. Role of reactive aldehyde in cardiovascular diseases. *Free Radical Biol. Med.* **28**, 1685–96 (2000).
- Uchida, K. 4-Hydroxy-2-nonenal: a product and mediator of oxidative stress. *Prog. Lipid Res.* **42**, 318–343 (2003).
- Wuttge, D. M. *et al.* T-cell recognition of lipid peroxidation products breaks tolerance to self proteins. *Immunology*. **98**, 273–279 (1999).
- Binder, C. J. & Silverman, G. J. Natural antibodies and the autoimmune of atherosclerosis. *Springer Semin Immunopathol.* **26**, 385–404 (2005).
- Stadtman, E. R. Protein oxidation and aging. *Science* **257**, 1220–1224 (1992).
- Stadtman, E. R. & Levine, R. L. Protein oxidation. *Ann. NY Acad. Sci.* **899**, 191–208 (2000).
- Kowal, C. L. *et al.* Molecular mimicry between bacterial and self antigen in a patient with systemic lupus erythematosus. *Eur. J. Immunol.* **29**, 1901–1911 (1999).
- Limpanasithikul, W. *et al.* Cross-reactive antibodies have both protective and pathogenic potential. *J. Immunol.* **155**, 967–973 (1995).
- Chan, T. M. *et al.* Mesangial cell-binding anti-DNA antibodies in patients with systemic lupus erythematosus. *J. Am. Soc. Nephrol.* **13**, 1219–1229 (2002).
- Jacob, L. *et al.* Presence of antibodies against a cell-surface protein, cross-reactive with DNA, in systemic lupus erythematosus: a marker of the disease. *Proc. Natl. Acad. Sci. U.S.A.* **84**, 2956–2959 (1987).
- Lee, S. H. & Blair, I. A. Characterization of 4-oxo-2-nonenal as a novel product of lipid peroxidation. *Chem. Res. Toxicol.* **13**, 698–702 (2000).
- Otaki, N. *et al.* Identification of a lipid peroxidation product as the source of oxidation-specific epitopes recognized by anti-DNA autoantibodies. *J. Biol. Chem.* **285**, 33834–33842 (2010).
- Witztum, J. L. & Steinberg, D. The oxidative modification hypothesis of atherosclerosis: Does it hold for humans? *Trends Cardiovasc. Med.* **11**, 93–102 (2001).
- Xu, G. & Sayre, L. M. Structural characterization of a 4-hydroxy-2-alkenal-derived fluorophore that contributes to lipoperoxidation-dependent protein cross-linking in aging and degenerative disease. *Chem. Res. Toxicol.* **11**, 247–251 (1998).
- Dragan, A. I. *et al.* SYBR Green I: fluorescence properties and interaction with DNA. *J. Fluoresc.* **22**, 1189–1199 (2012).
- Carter, D. C. & Ho, J. X. Structure of Serum Albumin. *Adv. Protein Chem.* **45**, 153–203 (1994).
- Rezwani, K. *et al.* Bovine serum albumin adsorption onto colloidal Al<sub>2</sub>O<sub>3</sub> particles: A new model based on zeta potential and UV-vis measurements. *Langmuir*. **20**, 10055–10061 (2004).
- Cosa, G. *et al.* Photophysical properties of fluorescent DNA-dyes bound to single- and double-stranded DNA in aqueous buffered solution. *Photochem. Photobiol.* **73**, 585–599 (2001).
- Radic, M. Z. & Weigert, M. Genetic and structural evidence for antigen selection of anti-DNA antibodies. *Annu Rev Immunol.* **12**, 487–520 (1994).
- Fink, H.-W. & Schönenberger, C. Electrical conduction through DNA molecules. *Nature* **398**, 407–410 (1999).
- Sayre, L. M. *et al.* Pyrrole formation from 4-hydroxynonenal and primary amines. *Chem. Res. Toxicol.* **6**, 19–22 (1993).
- Itakura, K., Osawa, T. & Uchida, K. Structure of a fluorescent compound formed from 4-hydroxy-2-nonenal and N<sup>ε</sup>-hippuryllysine: A model for fluorophores derived from protein modifications by lipid peroxidation. *J. Org. Chem.* **63**, 185–187 (1998).
- Hidalgo, F. J. & Zamora, R. Fluorescent pyrrole products from carbonyl-amine reactions. *J. Biol. Chem.* **268**, 16190–16197 (1993).
- Zhang, W.-H. *et al.* Model studies on protein side chain modification by 4-oxo-2-nonenal. *Chem. Res. Toxicol.* **16**, 512–523 (2003).
- Salomon, R. G. *et al.* Levuglandin E<sub>2</sub>-protein adducts in human plasma and vasculature. *Chem. Res. Toxicol.* **10**, 536–545 (1997).
- Hidalgo, F. J. & Zamora, R. Epoxyoxoene fatty esters: Key intermediates for the synthesis of long chain pyrrole and furan fatty esters. *Chem. Phys. Lipids.* **77**, 1–11 (1995).
- Salomon, R. G. *et al.* HNE-derived 2-pentylpyrroles are generated during oxidation of LDL, are more prevalent in blood plasma from patients with renal disease or atherosclerosis, and are present in atherosclerotic plaques. *Chem. Res. Toxicol.* **13**, 557–564 (2000).
- Kaur, K. *et al.* (Carboxyalkyl)pyrroles in human plasma and oxidized low-density lipoproteins. *Chem. Res. Toxicol.* **10**, 1387–1396 (1997).
- De Montarby, L., Mosset, P. & Gree, R. Sorbic acid iron tricarbonyl complex as resolving agent. Chiral syntheses of 4-hydroxy nonenal and coriolic acid. *Tetrahedron Lett.* **29**, 3895 (1988).
- Sun, M. *et al.* Novel bioactive phospholipids: practical total syntheses of products from the oxidation of arachidonic and linoleic esters of 2-lysophosphatidylcholine. *J. Org. Chem.* **67**, 3575–3584 (2002).
- Zamora, R., Navarro, J. L. & Hidalgo, F. J. Determination of lysine modification product epsilon-N-pyrrolylnorleucine in hydrolyzed proteins and trout muscle



microsomes by micellar electrokinetic capillary chromatography. *Lipids* **30**, 477–483 (1995).

## Acknowledgments

We thank Dr. Keiko Kuwata (Institute of Transformative Bio-Molecules (WPI-ITbM), Nagoya University) for technical assistance with nano-LC-ESI-Q-TOF-MS/MS analysis and Dr. Noritada Kaji (Nagoya University, Graduate School of Engineering) for technical assistance with Zeta potential analysis. We also thank Ms Yuki Hondoh for her excellent editorial support. This work was supported by grants from the Japan Society for the Promotion of Science (JSPS KAKENHI numbers: 20117007, 21248016, and 24658122); a grant from the JST A-step program; a grant from the JST PRESTO program; grants from the Ministry of Health, Labor and Welfare of Japan. A part of this work was conducted in Institute of Transformative Bio-Molecules (WPI-ITbM) at Nagoya University. This work was partly supported by Nanotechnology Platform Program (Molecule and Material Synthesis) of the Ministry of Education, Culture, Sports, Science and Technology (MEXT), Japan.

## Author contributions

K.U. designed and analyzed the experiments and wrote the paper. H.M., N.O., M.C., Y.H., F.N. and Y.S. performed the experiments. N.M. performed ionic conductivity study. T.H.

performed CD measurements. T.S. helped designed and analyzed the study. S.M. contributed reagents. H.M. and T.S. designed the experiments and edited the paper. All authors discussed the results and commented on the manuscript.

## Additional information

**Supplementary information** accompanies this paper at <http://www.nature.com/scientificreports>

**Competing financial interests:** The authors declare no competing financial interests.

**How to cite this article:** Miyashita, H. *et al.* Lysine pyrrolation is a naturally-occurring covalent modification involved in the production of DNA mimic proteins. *Sci. Rep.* **4**, 5343; DOI:10.1038/srep05343 (2014).



This work is licensed under a Creative Commons Attribution-NonCommercial-NoDerivs 4.0 International License. The images or other third party material in this article are included in the article's Creative Commons license, unless indicated otherwise in the credit line; if the material is not included under the Creative Commons license, users will need to obtain permission from the license holder in order to reproduce the material. To view a copy of this license, visit <http://creativecommons.org/licenses/by-nc-nd/4.0/>